Annals of Nuclear Medicine Vol. 10, No. 2, 185–191, 1996

FDG-PET in infectious lesions: The detection and assessment of lesion activity

Yuichi ICHIYA, Yasuo KUWABARA, Masayuki SASAKI, Tsuyoshi YOSHIDA, Yuko AKASHI, Sadayuki MURAYAMA, Katsumasa NAKAMURA, Toshimitsu FUKUMURA and Kouji MASUDA

Department of Radiology, Faculty of Medicine, Kyushu University

The usefulness of FDG-PET in the detection of infectious foci and the assessment of lesion activity was evaluated. The study covered 24 patients with 25 FDG-PET studies, including lesions of bacterial, tuberculous and fungal origins. The FDG uptake was determined by the lesion to muscle ratio (LMR) on the static images. The time activity curves (TACs) were classified into four patterns based on both the existence of an initial peak and a slope thereafter. A high FDG uptake was observed in 23 of 25 lesions (92%). Two lesions, in which no abnormal uptake was noted, included one in the healing stage and the other consisting of a cavity with a thin wall. The acute active lesions showed higher LMRs than the chronic active or healing lesions (mean ± SD: 9.8 ± 3.6, 3.6 ± 1.8 and 4.3 ± 1.7, respectively, $p < 0.05$), and they could be approximately distinguished by an LMR of 6. The patterns of the TACs in acute or chronic active lesions were either an increase without an initial peak or a plateau, while those in the healing lesions demonstrated predominantly an increase with an initial sharp peak. Our results indicated that FDG-PET is clinically useful in the detection of the infection of miscellaneous microorganisms as well as in the assessment of lesion activity.

Key words: ^{18}F-fluorodeoxyglucose, positron emission tomography, infectious disease, tuberculosis, abscess

INTRODUCTION

IT HAS BEEN REPORTED that ^{18}F-fluorodeoxyglucose (FDG) accumulates not only in malignant tumors but also in inflammatory lesions of both infectious and non-infectious origins, including brain abscesses,[1–3] pulmonary granuloma,[4,5] pulmonary histoplasmosis,[6] pulmonary tuberculosis,[7,8] pulmonary anthracosis,[5] posttherapy fibrosis in the lung,[9] sarcoidosis,[10] abdominal abscesses,[11,12] liver abscesses,[12] inflammatory pseudotumors of the liver,[12] chronic pancreatitis,[12] pelvic abscesses[12] and the post-irradiated state.[13] But these reports have mainly focused on the differential diagnosis of malignant and benign lesions, while there have been few reports to date regarding the role of FDG-PET in the evaluation of inflammatory lesions.[10,12] In this study, we evaluated the usefulness of FDG-PET in infectious lesions in respect to the detection of infectious foci and the assessment of lesion activity.

Received October 12, 1995, revision accepted January 16, 1996.

For reprint contact: Yuichi Ichiya, M.D., Department of Radiology, Faculty of Medicine, Kyushu University, Fukuoka 812–82, JAPAN.

MATERIALS AND METHODS

Patients

The study covered 24 patients with miscellaneous infectious lesions who underwent 25 FDG-PET studies (Table 1). One patient (case 2 in Table 1) underwent FDG-PET twice with an interval of 42 days. Details of 3 patients (cases 1, 2 and 4) were previously reported.[1,11] The final diagnoses were established by identification of the microorganisms in 10 patients, the clinical courses in 9, histology in 4 and necropsy in 1, and they were pulmonary tuberculosis in 8, pneumonia in 6, an abdominal abscess in 3 (with 4 FDG-PET studies), a liver abscess in 2, and brain abscess, tuberculous osteomyelitis, a pulmonary abscess, pulmonary atypical mycobacteriosis and pulmonary aspergillosis in 1, respectively. Fifteen patients had already received antibiotics at the time of the FDG-PET study. The inflammatory stages were determined on the

Table 1 Patient profiles

Case	Age/ Sex	Diagnosis	Causative organism	Method of diagnosis	Stage	Pattern	Size (cm)	LMR	TAC
1	52/M	Brain abscess	*Corynebacterium*	OP	AA	Focal	4	ND	NP
2	21/F	Abdominal abscess	n.i.	OP	AA	Focal	7 × 4	14.0	I
					H	Focal	6 × 3	5.1	II
3	26/F	Abdominal abscess	n.i.	OP	AA	Focal	10 × 3	13.3	I
4	41/M	Abdominal wall abscess	*Escherichia coli*	OP	AA	Focal	9 × 4	10.5	NP
5	56/F	Liver abscess	n.i.	CC	H	Focal	3	5.7	III
6	62/F	Liver abscess	n.i.	CC	H	Focal	3.5 × 2	Negative	NP
7	22/M	Tuberculous osteomyelitis	*Mycob. tbc*	OP	CA	Focal	7 × 4	6.3	I
8	72/M	Pulmonary abscess	*Pseudomonas*	Sputum	AA	Focal	5.5	6.1	I
9	67/M	Bronchopneumonia	n.i.	CC	AA	Infiltrative	5	5.3	I
10	72/F	Lobar pneumonia	n.i.	CC	H	Infiltrative	12	5.3	I
11	72/F	Organizing pneumonia	n.i.	CC	H	Focal	3	6.1	III
12	56/F	Organizing pneumonia	n.i.	CC	H	Focal	3	2.3	IV
13	55/F	Organizing pneumonia	n.i.	CC	H	Focal	3	4.1	III
14	66/M	Organizing pneumonia	n.i.	CC	H	Focal	4	4.4	III
15	44/M	Pulmonary tuberculosis	*Mycob. tbc*	Sputum	CA	Focal	2.5	Negative	NP
16	61/M	Pulmonary tuberculosis	*Mycob. tbc*	OP	CA	Focal	3	6.9	NP
17	64/M	Pulmonary tuberculosis	n.i.	CC	CA	Focal	3	3.1	NP
18	48/F	Pulmonary tuberculosis	n.i.	TBLB	CA	Focal	3	3.1	II
19	27/F	Pulmonary tuberculosis	*Mycob. tbc*	BL	CA	Focal	3.5	2.3	II
20	56/F	Pulmonary tuberculosis	n.i.	LNB	CA	Focal	4.5	3.4	II
21	24/F	Pulmonary tuberculosis	*Mycob. tbc*	Sputum	CA	Scattered	< 1	1.4	NP
22	20/M	Pulmonary tuberculosis	*Mycob. tbc*	Sputum	CA	Focal, scattered	< 4	4.8	I
23	50/M	Pulmonary atypical mycobacteriosis	*Mycob. avium*	Sputum	CA	Infiltrative	12	4.2	I
24	76/M	Pulmonary aspergillosis	*Aspergillus*	Necropsy	CA	Semi-invasive	12	3.4	I

n.i.: not identified, *Mycob. tbc*: *Mycobacterium tuberculosis*, *Mycob. avium*: *Mycobacterium avium* complex, OP: operation, CC: clinical course, TBLB: transbronchial lung biopsy, BL: bronchial lavage, LNB: lymph node biopsy, AA: acute active, CA: chronic active, H: healing, LMR: lesion to muscle ratio, ND: not determined, NP: not performed

basis of the clinical manifestations and the courses; namely, acute active: a progressive lesion with a duration of less than 1 month from onset; chronic active: a progressive lesion with a duration of more than 1 month from onset; and healing: a resolving lesion which still remains. They were determined to be in the acute active stage in 6 lesions, the chronic active stage in 11, and the healing stage in 8. The sizes of the lesions were determined by an X-ray CT.

The serum glucose values at the time of the PET study were measured on 18 PET studies. They were 94.3 ± 13.5 mg/d*l* (mean ± SD), ranging from 75 to 122 mg/d*l*. Serum insulin values were not measured. Two patients (cases 4 and 14) were known to have diabetes mellitus. Their serum glucose values were 122 mg/d*l* at the time of the PET study in case 14 and 116 mg/d*l* obtained 5 days after the PET study in case 4.

The investigation was approved by the committee for the medical application of the cyclotron-produced radionuclides in Kyushu University Hospital, and informed consent was obtained from all patients.

FDG-PET study

FDG was prepared as described previously.[14] A positron scanner SET130W (Shimadzu Corp. and Akita Noken, Japan) was used for the scanning, which has 3 detector rings providing 5 contiguous slices at 15 mm intervals. The effective spatial resolution used in the study was 14 mm in FWHM. Transmission scanning was performed with a $^{68}Ge/^{68}Ga$ ring source for attenuation correction. From 111 to 296 MBq (3–10 mCi) of FDG was slowly injected in a fasting state. Static scanning was done for 15 minutes from 45 to 60 minutes in all 25 PET studies. In addition, 17 serial scannings were also done over a 45-minute period from immediately after the injection in 18 PET studies. Matrices of 128 × 128 were used, with each pixel measuring 3 mm × 3 mm in size.

Data analysis

With reference to the X-ray CT images, PET images were visually interpreted by three nuclear medicine physicians depending on the existence of an abnormal FDG uptake in the lesion.

On the static images, the regions of interests (ROIs), which ranged from 15 mm × 15 mm to 27 mm × 27 mm in size, were placed on the lesion and muscles. The area showing the highest FDG uptake was chosen as the ROI of the lesion. The ROIs of the muscle were set on from 5

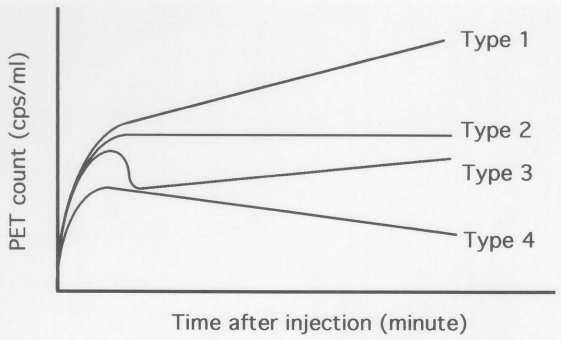

Fig. 1 The patterns of the time activity curves.

to 8 different parts, and their mean values were used. The lesion to muscle ratio (LMR) was calculated from the mean counts per volume in the lesion and the muscles, and was used as an index of the FDG uptake. The LMR could not be obtained in one patient (case 1), since the muscle component did not exist in the scanning field. The LMR in the lesions which were not identified on the FDG-PET images was assumed to be 1 in the following analysis.

The time activity curves (TACs) were obtained with the 18 scanning data from 0 to 60 minutes postinjection. Based on the existence of an initial peak within 10 minutes and changes of more than 20% in the PET counts from 10 to 60 minutes, the TACs were classified into four patterns: Type I, an increase up to 60 minutes; Type II, a plateau; Type III, an initial peak and then a gradual increase thereafter; and Type IV, a decrease (Fig. 1).

A combination of one way factorial ANOVA and Scheffe's multiple comparison test, and the chi-square test were used for the statistical analysis.

RESULTS

A high FDG uptake was noted in 23 out of 25 lesions (92%) (Figs. 2 through 5). Among them, a prominently high FDG uptake was noted in 3 with an abdominal abscess in the acute active stage. Two lesions showed no FDG uptake, and included one with a liver abscess in the healing stage measuring 3.5 cm in diameter and another with pulmonary tuberculosis consisting of a cavity with a thin wall measuring 2.5 cm in diameter. The sensitivities according to the inflammatory stages were 5/5 (100%) in the acute active stage, 12/13 (92%) in the chronic active stage and 8/9 (89%) in the healing stage.

The mean LMR in the acute active lesions was higher than that in the chronic active lesions (mean ± SD: 9.8 ± 3.6 versus 3.6 ± 1.8, $p < 0.05$) (Fig. 6). It was also higher than that in the healing lesions (the latter: 4.3 ± 1.7, $p < 0.05$). The active lesions were approximately distinguished by an LMR of 6 from the chronic active or healing lesions ($p < 0.05$, respectively) (Table 2). No difference was noted in the mean LMRs for the chronic active and healing lesions.

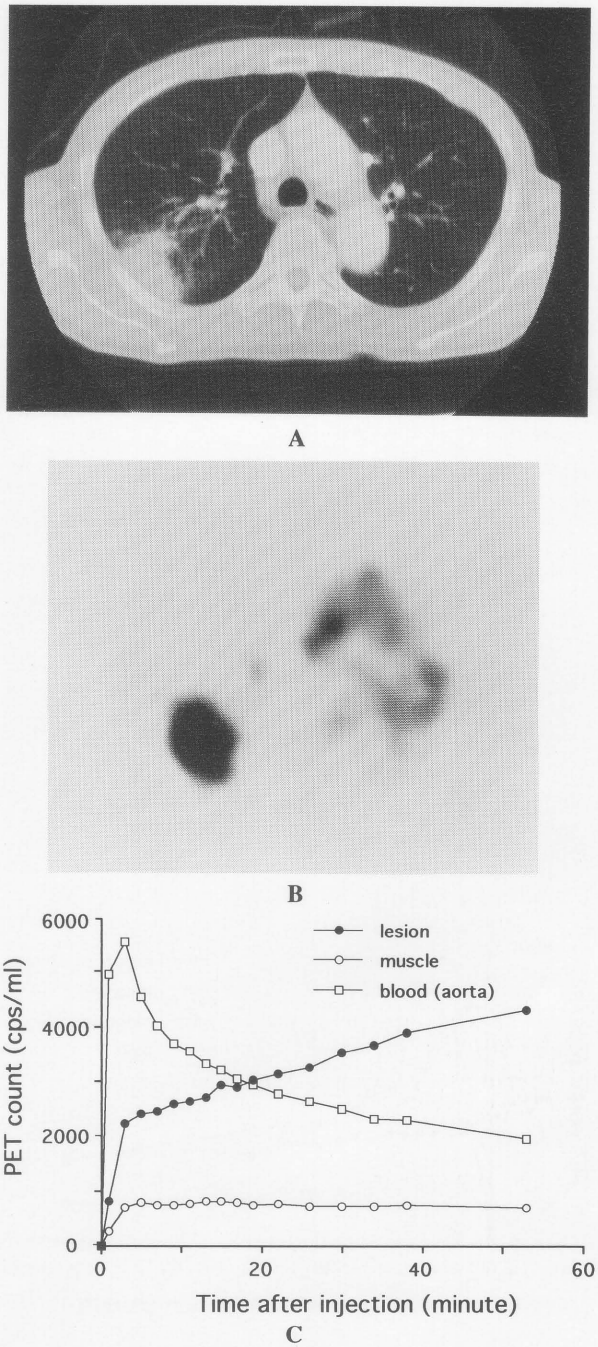

Fig. 2 A 72-year-old-male (Case 8) demonstrating a pulmonary abscess in the acute active stage. An enhanced CT (A) shows a consolidation with an ill-defined margin in the right posterior segment measuring 5.5 cm in size. On an FDG-PET image (B), a high FDG uptake is noted in the corresponding area with an LMR of 3.5. A high uptake is also noted in the enlarged mediastinal lymph nodes. The time activity curve (C) shows a Type I pattern.

In the analysis of the TACs, Type I was observed in 9 lesions, Type II in 4, Type III in 4 and Type IV in 1 (Table 3). After comparing the TAC and the lesion activity, the TACs in all 4 acute active lesions were Type I, while those in the chronic active lesions were either Type I or Type II.

A

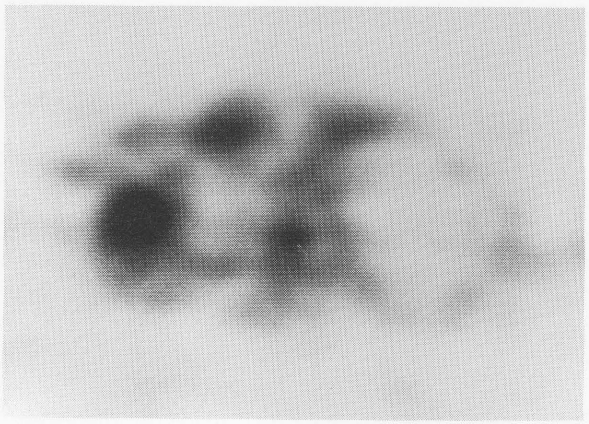

B

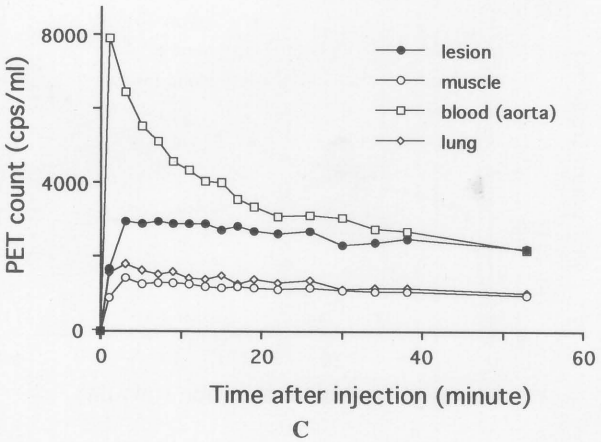

C

Fig. 3 A 27-year-old-female (Case 19) with pulmonary tuberculosis in the chronic active stage. A plain CT (A) shows fibrotic changes with a bullous formation in the right apical segment. Adjacent pleural thickening is also noted. The findings on CT are suggestive of a healed scar from tuberculosis. However, on an FDG-PET image (B), a high uptake is noted with an LMR of 2.3, and the time activity curve (C) shows a Type II pattern. Tuberculous bacilli were identified by transbronchial lavage, and thereafter anti-tuberculous medication was administered. The lesion had decreased in size 6 months later.

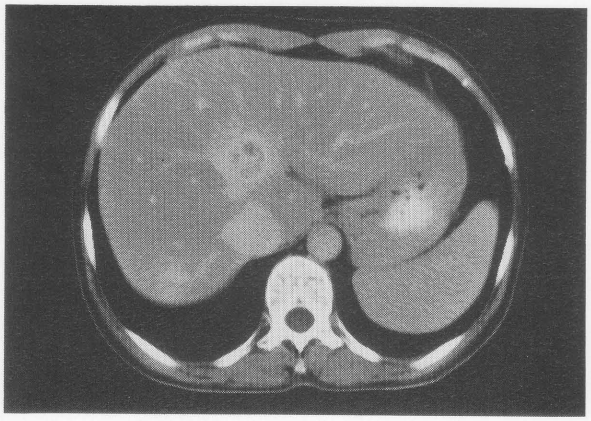

A

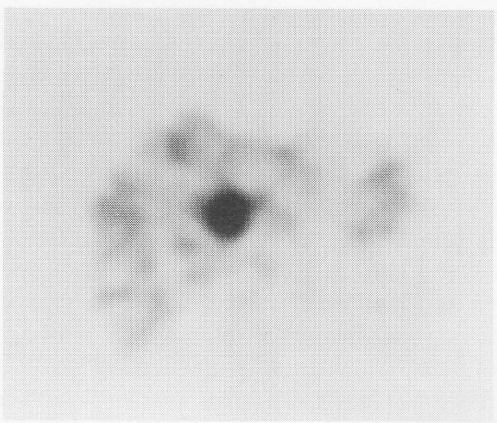

B

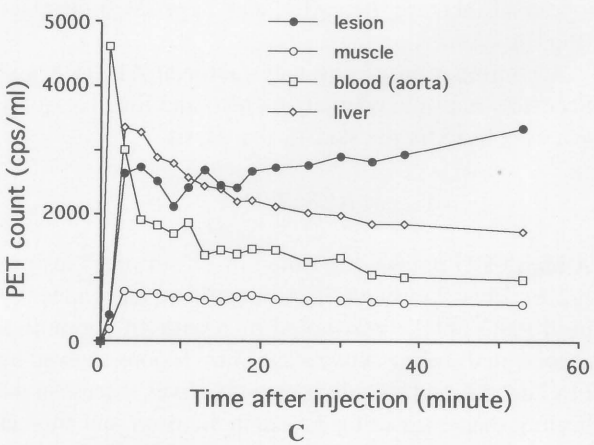

C

Fig. 4 A 56-year-old-female (Case 5) presenting with a liver abscess in the healing stage. An enhanced CT (A) shows a round low density mass with a ring-like enhancement in the medial segment of the left lobe measuring 3 cm in diameter. On an FDG-PET image (B), a high FDG uptake is noted in the corresponding area showing an LMR of 5.7. The normal liver is also faintly visualized. The time activity curve (C) shows a Type III pattern.

In contrast to this, the healing lesions were predominantly Type III, although the remaining 3 types were also noted on occasion.

DISCUSSION

The sites of FDG accumulation in infectious lesions are considered to be in migratory inflammatory cells,[15–18] causative microorganisms[19] and granulation tissue.[20,21] It

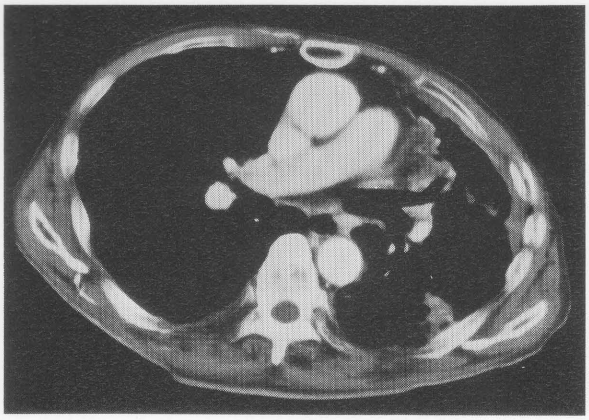

A

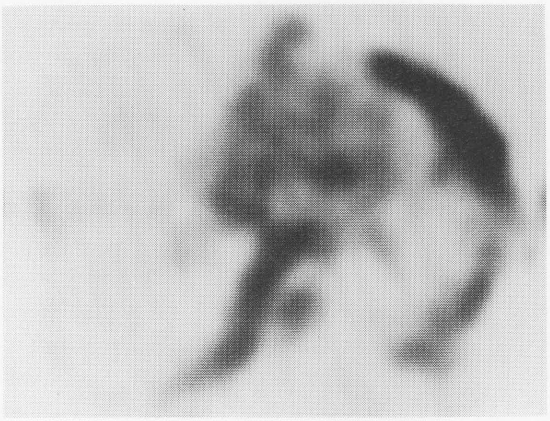

B

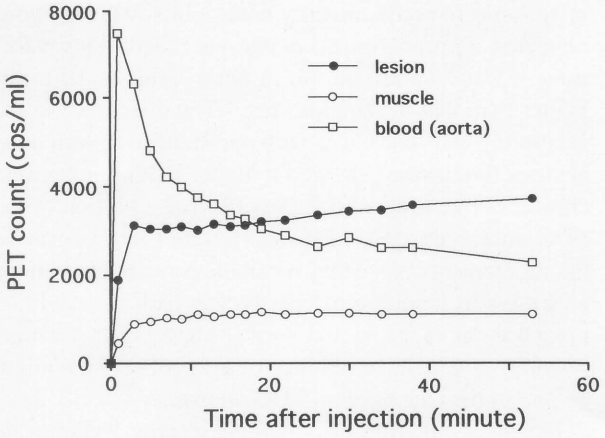

C

Fig. 5 A 76-year-old-male (Case 24) with bilateral pulmonary aspergillosis in the chronic active stage. The patient had been diagnosed with aspergillosis 6 years before. An enhanced CT (A) shows a large cavitary lesion containing a fungus ball in the left upper lobe. The adjacent chest wall is also involved. On an FDG-PET image (B), the FDG uptake is not uniform in the lesion, and the highest uptake is observed in the left anterior chest wall showing an LMR of 3.4. A high uptake is also noted in the right pleural lesion. The time activity curve (C) shows a Type II pattern.

Table 2 Comparison of the lesion activities and FDG uptake

	LMR	
	More than 6	Less than 6
Acute active*,** (n = 5)	4	1
Chronic active* (n = 11)	2	9
Healing** (n = 8)	1	7

*: $p < 0.05$, **: $p < 0.05$

Table 3 The correlation of the inflammatory stages and the patterns of the time activity curve (n = 18)

	Patterns of TAC			
	I	II	III	IV
Acute active (n = 4)	4	0	0	0
Chronic active (n = 7)	4	3	0	0
Healing (n = 7)	1	1	4	1

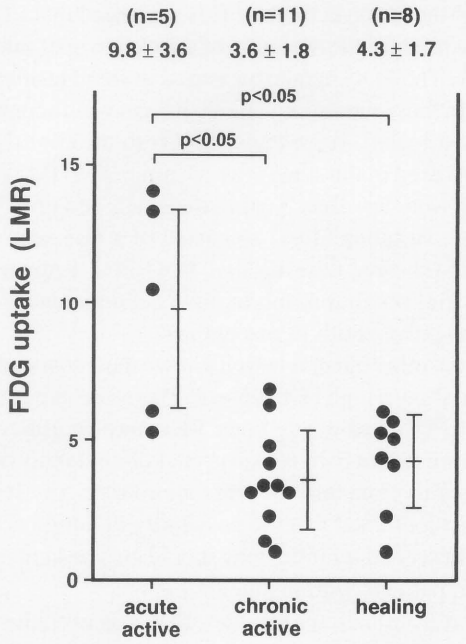

Fig. 6 The FDG uptake according to the lesion activity.

is considered that the former two play a predominant role in the acute stage, while the last one plays a role in the healing stages. It is known that neutrophils utilize glucose as a source of energy, and even in aerobic conditions they derive most of their energy supply from glycolysis. FDG uptake reflects the glucose metabolism in the process of both the transport of glucose into the cells and the conversion to glucose-6-phosphate.[22] FDG uptake is therefore further accelerated in anaerobic glycolysis, compared to that in aerobic metabolism. Infiltrating cells in acute

infections are predominantly neutrophils, whereas lymphocytes are predominant in chronic tuberculous infections.[23] Glucose utilization in neutrophils is 10 times higher than that in lymphocytes.[15] The difference in the infiltrating cells correlates with our findings in which the acute active lesions showed a higher FDG uptake than chronic active lesions. It is possible that a portion of the FDG administered is also incorporated into causative microorganisms, since they metabolize glucose in various pathways as a source of energy.[19] A lack of any FDG uptake in an experimental aseptic abscess has been reported,[22] in which the absence of microorganisms might be one of the causes of no FDG uptake.

For the evaluation of infectious lesions, ^{67}Ga-citrate (Gallium) and ^{111}In-leukocyte (In-WBC) have been used widely in clinical practice.[24–30] The uptake mechanism of these agents differs from that of FDG. Gallium is incorporated in migratory white blood cells, causative microorganisms and binding sites with lactoferrin.[24,25] In-WBC simply reflects the distribution of migratory white blood cells.[30] Regarding comparisons between the two agents, it has been reported that In-WBC is less sensitive in chronic or healing lesions, whereas Gallium may fail to detect acute lesions.[26] It has also been reported that In-WBC may produce a negative scan in fungal or parasitic infections.[27] These differences also correlate with the difference in their mechanisms of the accumulation.

In this series, high FDG uptake was noted in 23 out of 25 lesions regardless of either the causative microorganisms or the lesion activities. This suggested that FDG can thus be used for the detection of a wide range of infectious lesions. The FDG uptake measured in small lesions especially in those measuring less than 3 cm was thought to be underestimated, since the spatial resolution of the PET scanner used in the study was 14 mm in FWHM.[31,32] Two lesions were less than 3 cm in diameter, and one of them with active tuberculosis consisted of a thin-wall cavity (case 15) showed false negative FDG-PET. Limitations in the spatial resolution might have been the cause of the false negative result in this patient.

On the other hand, it is well known that most malignant tumors show a high FDG uptake. Therefore, the combination of FDG and whole body PET may be utilized as a screening test in patients suspected of an unknown focal abnormality from infectious or tumorous origins. It should also be mentioned that the possibility of a high accumulation in secondary infections should also be kept in mind even in patients with malignant tumors.[14,18]

Apart from such sensitivities, FDG has two advantages in the detection of infectious lesions when compared to the above mentioned agents. The first is short examination time. When Gallium or In-WBC is used, at least 4–6 hours, or ideally 24 hours postinjection, are required before scanning. FDG has fast uptake in lesions as well as fast clearance from the blood, which makes it possible for FDG-PET to be completed within 1 hour postinjection. This is especially advantageous in the diagnosis of acute infections. The second advantage is that the physiological accumulation of FDG is confined to the brain and heart, while little uptake is noted in the abdominal organs such as the liver and urinary tract. Gallium shows high accumulation in the liver and bowel, and In-WBC in the liver and bone marrow. These physiological accumulations may interfere with detection in either the superimposed or surrounding areas. In this regard, FDG is therefore considered to be superior in the diagnosis of abdominal lesions.

Regarding the assessment of lesion activity, the LMRs differentiated the acute active lesions from both chronic active and healing lesions. However, no difference was observed between chronic active and healing lesions. In addition to the LMRs, the TACs also afforded additional information in the assessment of lesion activities. In this series, Type I and II patterns were observed in the active lesions, and Type III and IV patterns were observed in healing lesions. It is interesting to note that the patterns of the TACs observed in this series were similar to those found in malignant tumors.[14,33] The TAC of Type I observed in the acute or chronic active stage was exactly the same as that in malignant tumors before therapy, whereas Types II and IV were observed after effective therapy. Minn et al.[33] analyzed the TACs in malignant tumors after therapy and classified them into three patterns, based on both a fast initial component and a following slow component. They speculated that a slow component reflected the tumor activity, while a fast initial component represented the blood flow rather than the tumor metabolism. It is therefore considered that the initial peak observed in this series represented a vascular component, which is not used for metabolism, resulting from increased blood flow due to newly-formed or dilated blood vessels. Thus, the Type III pattern, showing an initial peak and then a gradual increase thereafter, suggested the co-existence of both active and necrotic areas. In this series, this pattern was only noted in healing lesions, and was also helpful in differentiating between chronic active and the healing stages.

In conclusion, our results indicated that FDG-PET can be successfully used in the detection of infectious lesions as well as in the evaluation of lesion activity. It should also be kept in mind that secondary infections may cause false positive results in the interpretation of FDG-PET in patients with malignant tumors.

ACKNOWLEDGMENTS

The authors thank Drs. Kenji Kawatomo and Toshihiko Ueyama for their valuable suggestions, Mr. Brian T. Quinn for his editorial support and Ms. Miwa Watanabe for her secretarial assistance. This work was supported in part by a grant-in-aid for Cancer Research (06282110) from the Ministry of Education, Science and Culture, Japan.

REFERENCES

1. Sasaki M, Ichiya Y, Kuwabara Y, Otsuka M, Tahara T, Fukumura T, et al. Ringlike uptake of [^{18}F]FDG in brain abscess: A PET study. *J Comp Assist Tomogr* 14: 486–487, 1990.
2. Hanson MW, Glantz MI, Hoffman JM, Friedman AH, Burger PC, Schold SC, et al. FDG-PET in the selection of brain lesions for biopsy. *J Comp Assist Tomogr* 15: 796–801, 1991.
3. Meyer MA, Frey KA, Schwaiger M. Discordance between F-18 fluorodeoxyglucose uptake and contrast enhancement in a brain abscess. *Clin Nucl Med* 18: 682–684, 1993.
4. Kubota K, Matsuzawa T, Fujiwara T, Ito M, Hatazawa J, Ishiwata K, et al. Differential diagnosis of lung tumor with positron emission tomography: A prospective study. *J Nucl Med* 31: 1927–1933, 1990.
5. Wahl RL, Quint LE, Greenough RL, Meyer CR, White RI, Orringer MB. Staging of mediastinal non-small cell lung cancer with FDG PET, CT, and fusion images: Preliminary prospective evaluation. *Radiology* 191: 371–377, 1994.
6. Dewan NA, Gupta NC, Redepenning LS, Phalen JJ, Frick MP. Diagnostic efficacy of PET-FDG imaging in solitary pulmonary nodules. *Chest* 104: 997–1002, 1993.
7. Patz EF Jr, Lowe VL, Hoffman JM, Paine SS, Burrowes S, Coleman RE, et al. Focal pulmonary abnormalities: Evaluation with F-18 fluorodeoxyglucose PET scanning. *Radiology* 188: 487–490, 1993.
8. Strauss LG, Conti PS. The application of PET in clinical oncology. *J Nucl Med* 32: 623–648, 1991.
9. Patz EF Jr, Lowe VL, Hoffman JM, Paine SS, Harris LK, Goodman PC. Persistent or recurrent bronchogenic carcinoma: Detection with PET and 2-[F-18]-2-deoxy-D-glucose. *Radiology* 191: 379–382, 1994.
10. Brudin LH, Valind S-O, Rhodes CG, Pantin CF, Sweatman M, Jones T, et al. Fluorine-18 deoxyglucose uptake in sarcoidosis measured with positron emission tomography. *Eur J Nucl Med* 21: 297–305, 1994.
11. Tahara T, Ichiya Y, Kuwabara Y, Otsuka M, Miyake Y, Gunasekera RD, et al. High [F-18]-fluorodeoxy-glucose uptake in abdominal abscesses: A PET study. *J Comp Assist Tomogr* 13: 829–831, 1989.
12. Okazumi S, Enomoto K, Fukunaga T, Kikuchi T, Asano T, Isono K, et al. Evaluation of the cases of benign disease with high accumulation on the examination of F-18 fluorodeoxyglucose PET. *KAKU IGAKU (Jpn J Nucl Med)* 30: 1439–1443, 1993 (in Japanese).
13. Haberkorn U, Strauss LG, Dimitrakopoulou A, et al. PET studies of fluorodeoxyglucose metabolism in patients with recurrent colorectal tumors receiving radiotherapy. *J Nucl Med* 32: 1485–1490, 1991.
14. Ichiya Y, Kuwabara Y, Otsuka M, Tahara T, Yoshikai T, Fukumura T, et al. Assessment of response to cancer therapy using Fluorine-18-fluorodeoxyglucose and positron emission tomography. *J Nucl Med* 32: 1655–1660, 1991.
15. West J, Morton DJ, Esmann V, Stjernholm RL. Carbohydrate metabolism in leukocytes. VIII. Metabolic activities of the macrophage. *Archive Biochem Biophys* 124: 85–90, 1968.
16. Borregaard NB, Herlin T. Energy metabolism of human neutrophils during phagocytosis. *J Clin Invest* 70: 550–557, 1982.
17. Weisdorf DJ, Craddock PR, Jacob HS. Glycogenolysis versus glucose transport in human granulocytes: Differential activation in phagocytosis and chemotaxis. *Blood* 60: 888–893, 1982.
18. Daley JM, Shearer JD, Mastrofrancesco B, Caldwell MD. Glucose metabolism in injured tissue: A longitudinal study. *Surgery* 107: 187–192, 1990.
19. Anderson RL, Wood WA. Carbohydrate metabolism in microorganisms. *Ann Rev Microbiol* 23: 539–578, 1969.
20. Tischler ME, Fagan JM. Response to trauma of protein, amino acid, and carbohydrate metabolism in injured and uninjured rat skeletal muscles. *Metabolism* 32: 853–868, 1983.
21. Kubota R, Yamada S, Kubota K, Ishiwata K, Tamahashi N, Ido T. Intratumoral distribution of Fluorine-18-fluorodeoxyglucose *in vivo*: High accumulation in macrophages and granulation tissues studies by microautoradiography. *J Nucl Med* 33: 1972–1980, 1992.
22. Som P, Atkins HL, Bandoypadhyay D, Fowler JS, MacGregor RR, Matsui K, et al. A fluorinated glucose analog, 2-fluoro-2-deoxy-D-glucose (F-18): Nontoxic tracer for rapid tumor detection. *J Nucl Med* 21: 670–675, 1980.
23. Marchesi VT. Inflammation and healing. *In* Anderson's Pathology, Kissane JM (ed.), 8th ed., Mosby, pp. 22–60, 1985.
24. Staab EV, McCartney WH. Role of Gallium 67 in inflammatory Disease. *Sem Nucl Med* 8: 219–234, 1978.
25. Hoffer P. Gallium: Mechanisms. *J Nucl Med* 21: 282–285, 1980.
26. Sfakianakis GN, Al-Shikh W, Heal A, Rodman G, Zeppa R, Serafini A. Comparisons of scintigraphy with In-111 leukocytes and Ga-67 in the diagnosis of occult sepsis. *J Nucl Med* 23: 618–626, 1982.
27. Goodwin DA. Clinical use of In-111 leukocyte imaging. *Clin Nucl Med* 8: 36–38, 1983.
28. Kipper MS, Williams RJ. Indium-111 white blood cell imaging. *Clin Nucl Med* 8: 449–455, 1983.
29. Datz FL, Thorne DA. Effect of chronicity of infection on the sensitivity of the In-111-labeled leukocyte scan. *AJR* 147: 809–812, 1986.
30. Froelich JW, Swanson D. Imaging of inflammatory processes with labeled cells. *Sem Nucl Med* 14: 128–140, 1984.
31. Kuwert T, Ganslandt T, Jansen P, et al. Influence of size of regions of interest on PET evaluation of caudate glucose consumption. *J Comput Assist Tomogr* 16: 789–794, 1992.
32. Akashi Y, Kuwabara Y, Ichiya Y, Sasaki M, Yoshida T, Fukumura T, et al. The partial volume effect correction for pulmonary mass lesions using a ^{68}Ga/^{68}Ge transmission scan in PET study. *KAKU IGAKU (Jpn J Nucl Med)* 31: 1511–1517, 1994 (in Japanese).
33. Minn H, Paul R, Ahonen A. Evaluation of treatment response to radiotherapy in head and neck cancer with Fluorine-18 fluorodeoxyglucose. *J Nucl Med* 29: 1521–1525, 1988